ASHRAE and IBPSA-USA SimBuild 2016
Building Performance Modeling Conference
Salt Lake City, UT
August 8-12, 2016

CFD ANALYSIS OF NATURAL VENTILATION OF AN ISOLATED GENERIC BUILDING WITH A WINDWARD WINDOW AND A VENTURI-SHAPED WINDEXCHANGER

J. Antonio Castillo[1] and Guadalupe Huelsz[1]
[1]Instituto de Energías Renovables, Universidad Nacional Autónoma de México,
Priv. Xochicalco s/n Col. Centro, Temixco Morelos, México.

ABSTRACT

A windexchanger (WE) is a relatively small structure located on the building rooftop used to increase the wind driven natural ventilation. In this work, the use a Venturi-shaped roof for the square-cross-section WE with one duct and four openings to further increase the natural ventilation in a room is proposed. Computational Fluid Dynamics (CFD) simulations, experimentally validated, are used to study the impact of this Venturi-shaped windexchanger (VESWE) on the natural ventilation in an isolated generic room with a windward window and incide wind normal to one of the VESWE openings. The VESWE performance is compared with that of the similar WE but with flat roof. For these conditions, it is concluded that, due to the competition of the Venturi and wind-blocking effects, there exist an optimal contraction ratio (high at the contraction/high at the roof perimeter) of the VESWE that gives the larger volumentric flow rate. The variation of the roof thickness of the VESWE does not give a so clear result, showing that the VESWE geometry has a complex interaction with the window at windward. The volumetric flow rate can increase up to 12% with respect to that of the similar WE with flat roof.

INTRODUCTION

Natural ventilation on buildings by wind driven flows is an important passive strategy to promote indoor air quality, hygrothermal comfort and health; mainly in warm climates. In Mexico, more than 70% territory has warm climates, and most of the dwellings that are being constructed are one or two floors, with only one opening per room. In these cases, the cross ventilation by two windows in opposite walls of a room is not viable. Thus alternatives based on ventilation through the roof can be used, this takes advantage that the roof is often the most exposed part of the dwelling to the wind (Blocken et al. 2011; van Hooff et al. 2011). A windexchanger (WE) is a relatively small structure located on the building rooftop, this structure is more commonly referred into the literature as windcatcher, but the term windexchanger accounts for the fact that this structure can act as an injector or extractor of air depending on orientation when the room has another opening (Cruz-Salas, Castillo, and Huelsz 2014; Su et al. 2008; Liu, Mak, and Niu 2011) or acts simultaneously as an injector and extractor when it has no other opening (Su et al. 2008; Li and Mak 2007; Elmualim and Awbi 2002; Elmualim 2006a; Elmualim 2006b). The construction of a WE to enhance natural ventilation is cheap compared with the total cost of the low-income dwellings that are being built in Mexico.

In all studies to evaluate WE, the WE has been placed on the roof of an isolated, generic building consisting of a single room, in all but (Khodakarami and Aboseba 2015), the WE is centered on the roof, and having itself a flat rooftop. Most of the WE studies are performed under different conditions hindering comparison between them (Khan, Su, and Riffat 2008; Montazeri and Azizian 2008; Hughes and Ghani 2010; Montazeri et al. 2010; Montazeri 2011; Saadatian et al. 2012). However, there are some studies that compare in the same conditions similar WE only changing the cross-section, rectangular or circular, these studies show that the rectangular one provides higher airflow rate than that with circular cross-section (Elmualim and Awbi 2002; Montazeri 2011). Recently, an experimental study compares in the same conditions different square-cross-section WE when used in a room with a windward window (Cruz-Salas, Castillo, and Huelsz 2014). The square-cross-section WE without divisions, *i.e.* with only one duct, and four openings, one per side, shows to produced relative high ventilation flow rate and high percentage area with a significant speed when the window is at windward, having better performance than a similar one but with four subducts.

A Venturi-shaped roof, named VENTEC has been propose by (Bronsema 2010) to promote natural ventilation in buildings. The VENTEC roof consists of a disc-shaped roof construction that is located at a given height above the actual building roof that also has a disc-shape. This creates a contraction that is expected to provide significant negative pressure due to the so-called Venturi-effect (Blocken et al. 2011). Parametric studies of the VENTEC roof on a high building, without an opening in the building roof, are conducted by (Blocken et al. 2011; van Hooff et al. 2011). Their studies show that the negative pressure in the roof does not monotonically decrease with increasing the contraction ratio (high at the contraction/high at the disc perimeter) and that an optimum contraction ratio exists. The reason is that a smaller

contraction ratio leads to a higher flow resistance through the contraction, which causes more flow over and around the roof rather than through the contraction. This wind-blocking effect is present in contractions in non-confined flows (Blocken, Stathopoulos, and Carmeliet 2008).

In this paper, it is proposed to use a Venturi-shaped roof for the square-cross-section windexchanger with one duct and four openings to further increase the natural ventilation in a room. Computational Fluid Dynamics (CFD) simulations, with the commercial software COMSOL 5.1, are used to study the impact of this Venturi-shaped windexchanger (VESWE) on the natural ventilation in an isolated generic room with a windward window. The generic room represents a room of the Mexican low-income dwellings where the VESWE could have a wide technical application. To compare the VESWE performance, the similar WE but with flat roof is used as the reference case. The CFD simulations were validated with experimental results reported by (Cruz-Salas, Castillo, and Huelsz 2014) for the WE with flat roof.

WINDEXCHANGER REFERENCE CASE

The WE reference case has square-cross-section, one duct, four openings and flat roof. It is located on the center of a room roof. The WE has a height of 1.40 m measured from the roof, have a square-cross-section of 0.65 m in length and it is designed with a roof eave of 0.64 m as solar and rain protection. The interior dimensions of the room are W $\times$ D $\times$ H $=$ 3.0 $\times$ 3.0 $\times$ 2.7 m^3. The room has a square window at windward, 1.30 m in length, giving a wall porosity (opening area divided by wall area) of 17% (Etheridge 2012), it is centered on the wall and its base is at a height of 0.90 m from the floor.

EXPERIMENTS

The room with the WE reference case was experimentally tested by (Cruz-Salas, Castillo, and Huelsz 2014) using a scaled model (1:25), as shown in Fig. 1. The scaled model was set in the test section of an open water channel (OWC) and Stereo Particle Image Velocimetry (SPIV) measurements were carried out. The OWC is 6 m long and has a test section of 1.0 $\times$ 0.315 $\times$ 0.41 m^3. The scaled model is made of transparent acrylic, with thicknesses of 6 mm for walls and room's roof, 9 mm for the floor, and 3 mm for the WE roof. The interior dimensions are W $\times$ D $\times$ H $=$ 12 $\times$ 12 $\times$ 10.8 cm^3. The SPIV measurements were performed in the vertical central plane, as shown in Fig. 1b. In the OWC, an atmospheric boundary layer (open-terrain roughness profile) of a suburban area was reproduced. The mean velocity U and turbulence intensity I profiles were measured in the empty test section at the model position but without it, *i.e.* incident profiles. The obtained friction coefficient of the exponential law is $\alpha = 0.29$ (Bañuelos Ruedas, Angeles-Camacho, and Rios-

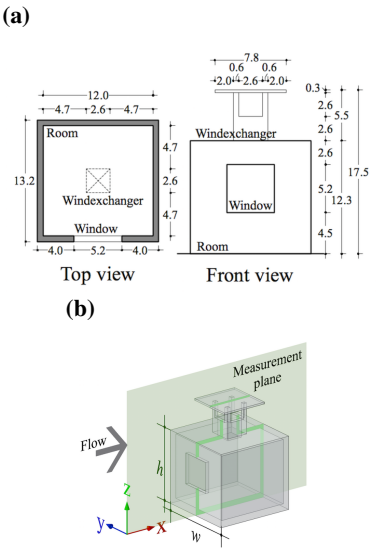

Figure 1: Model of the room with the windexchanger reference case. (a) Top and front view, units in centimeters; (b) Isometric view with the measurement plane and flow direction, where $h = 0.123$ m and $w = 0.132$ m are the external height and width of the room model, respectively.

Marcuello 2010) and the aerodynamic roughness length z_0 is 0.06 cm (for full scale, 0.015 m) (Wieringa 1992). The incident profiles are used for a reliable validation study as recommended by (Blocken, Stathopoulos, and Carmeliet 2008). A reference mean wind speed $U_{ref} =$ 0.089 m/s (for full scale, 0.062 m/s) and a reference turbulence intensity of 20% were measured at the reference height z_{ref} taken as the external height of the room $h =$ 12.3 cm (for full scale, 3.075 m). The experiments were made in water applying the dynamic similarity with the Reynolds number $Re = U_{ref} z_{ref}/\nu = 1.23 \times 10^4$, where $\nu = 8.94 \times 10^{-7}$ m^2/s is the kinematic viscosity at the water temperature $T_w = 25\ ^oC$.

CFD VALIDATION

The present paper reports a CFD study performed with the commercial code COMSOL 5.1 (COMSOL 2013). This section presents the simulation model and settings for the validation of the room with the WE reference case. The settings are taken from a previous validation work (Castillo, Huelsz, and Cruz 2014) using the experiments reported by (Cruz-Salas, Castillo, and Huelsz 2014) and succinctly presented in previous section.

Model and settings

For the CFD simulations, the 3D steady RANS equations in combination with the shear-stress transport (SST) k-ω model are solved. The GMRES solver with MULTIGRID-SOR preconditioner is employed for velocity-pressure coupling, and the MULTIGRID-SCGS

preconditioner is used for viscous terms of the governing equations (COMSOL 2013). The convergence criteria is assumed to be obtained when all the scaled residuals are equal or less than10^{-4}.

Computational domain and grid

The computational domain with the room with the WE reference case is developed following the best guidelines by (Tominaga et al. 2008; Ramponi and Blocken 2012), its dimensions are $W_d \times L_d \times H_d = 0.315 \times 2.346 \times 0.41$ m^3 (Figure 3a). A tetrahedral grid is created with 1,176,225 nodes (Figure 3b).

Boundary conditions

The inlet boundary conditions are set according to the experimental velocity and turbulent profiles. The velocity profile is defined by the logarithmic law, $U(z) = (u^*_{ABL}/\kappa) ln((z+z_0)/z_0)$, with the atmospheric boundary layer (ABL) friction velocity, $u^*_A BL = 0.007$ m/s, the von Karman constant, κ = 0.42, the roughness length, z_0 = 0.0005 m, and the height coordinate, z. The turbulent kinetic energy profile, $k(z) = (\sigma_u 2(z) + \sigma^2_v(z) + \sigma^2_w(z))/2$, is calculated from the standard deviation of each velocity component for x-direction, σ_u, for y-direction, σ_v, and for z-direction, σ_w. The turbulence dissipation rate and specific dissipation rate profiles are obtained, $\varepsilon(z) = u^{*3}_{ABL}/\kappa(z+z_0)$ and $\omega(z) = \varepsilon(z)/C_\mu k(z)$, respectively, with the empirical constant C_μ = 0.09 (Tominaga et al. 2008). The standard wall functions (COMSOL 2013) are set at ground surface and at lateral walls. The zero static pressure is applied on the rear face of the domain. The free slip condition at the top boundary is used to simulate the air-water interface. In Fig. 3, the velocity profile and turbulent profiles, $k(z)$ and $\omega(z)$ at the inlet and incident building position in the empty domain are presented, showing that their streamwise gradients are negligible.

Validation

In Fig. 4, the experimental and CFD velocity vector fields at the central plane are shown, as well as the streamwise speed ratio, u/U_{ref}, along an horizontal line, L_h. The CFD sumulations results show good agreement whit the SPIV experimental results. The averaged difference of streamwise speed ratios is lower than 10%.

VESWE EVALUATION

To evaluate the effect of the VESWE on natural ventilation in an isolated generic room with a windward window, the computational model presented in the previous sections are employed. Note that, the validated case simulates the experimental conditions: the distance of the lateral walls and the air-water interface. Those conditions can influence the dynamic of the ventilation on the room. To reduce these effects and to obtain a more reliable result a new domain is created by following the guidelines by (Franke et al. 2007; Tominaga et al. 2008), where the lateral and the top distances from the exterior surface of the room to the lateral and top boundaries, respectively, are five times of the characteristic length ($5 \times h$), see Figure 5. For these extended boundaries the symmetry boundary condition is employed. Additionally, the domain is rescaled to full scale and air used as working fluid (Partridge and Linden 2013). In that respect, the inlet vertical profiles of U, $k(z)$, $\varepsilon(z)$ and $\omega(z)$ are calculated by applying the dynamic similarity. The values for the full scale are $U_{ref} = 1.5$ m/s, $z_{ref} = h = 3.075$ m, $u^*_{ABL} = 0.095$ m/s, and $z_0 = 0.03$ m.

VESWE contraction height

In Fig. 6, the reference case, RC and the VESWE, V, with different contraction heights, c, are shown. The different values of c are obtained by vertically translating the Venturi shaped roof of the WE. The roof thickness, e, are 0.075 m and 0.20 m for the RC, and for the Venturi-shaped roofs respectively. In Table 1, the studied cases are presented. To evaluate the natural ventilation generated by each case, the normalized velocity magnitude U_m/U_{ref} and the pressure coefficient Cp are calculated in the vertical central plane. The pressure coefficient, $Cp = (P - P_{ref})/(0.5 * \rho U^2_{ref})$, is calculated with the the total pressure, P, the reference hydrostatic pressure, P_{ref}, and the air density, $\rho = 1.1839$ kg/m^3, at 25^oC. In addition, the volumetric flow rate, Q, through the window is calculated. In Fig. 6, the contour plots of the U_m/U_{ref} and Cp are shown. It can be observed that the velocity magnitude distribution inside the room has: an incoming jet from the room window to the interconection of the room and the WE; and a low velocity zone in the center and in the rear area of the room. For the cases V_C3, V_C4 and V_C5, the incoming jet has the greatest normalized velocity magnitude values. For these three cases, the contraction height c produces the optimal combination between the Venturi-effect and the wind-blocking-effect. The narrow contraction zone, *i.e.* a negative pressure zone, balances the incoming flows (through the window and the VESWE entrance opening, both at windward) with the outflows (through the room-VESWE interconnection and the VESWE exit openings at leeward). These observations can be confirmed by the Cp difference between the windward facade of the room and the VESWE contraction zone, shown in Figure 6. V_C4 shows the maximum underpressure. Table 2 presents the volumetric flow rate, Q, through the window of the room when its rooftop has one of the VESWEs. It can be observed that Q is improved by V_C4 in 11%, while is reduced in 17% by V_C1, with respect to RC.

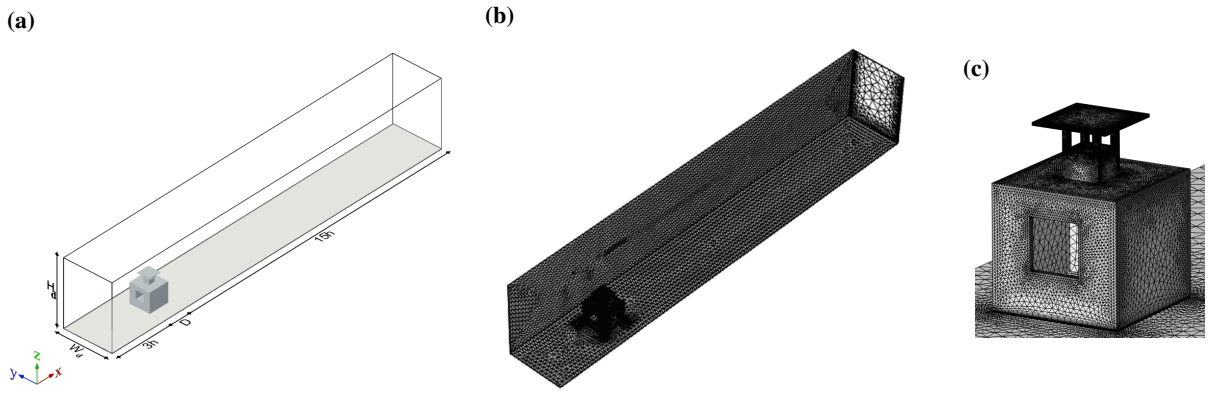

Figure 2: Computational domain with the model of the room with the WE reference case: (a) Perspective view with dimensions of the domain; (b) Perspective view of grid at bottom face (grid A with 1,176,225 nodes); (c) Isometric view of the room with the WE reference case.

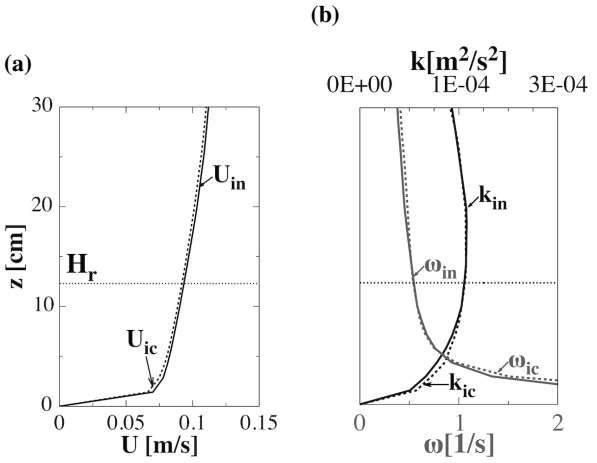

Figure 3: Vertical profiles of (left) the mean velocity, U; (right) the turbulent kinetic energy (dark line), k, and the specific dissipation rate (gray line), ω, at the inlet (continuous line) and at the incident building position (dashed line) in the empty domain. The subscripts in and ic refer to inlet and incident, respectively. The height of the model (h) is 0.123 m.

Table 1: Venturi-shaped windexchanger cases with parameters. The letters e, c, b and b/c indicate the roof thickness, the height contraction, the height from the WE sill to the WE rooftop, and the the contraction ratio, respectively.

Cases	e [m]	c [m]	b [m]	b/c [-]
RC	**0.08**	**0.65**	**0.73**	**1.12**
V_C1	0.20	0.16	0.36	2.23
V_C2	0.20	0.33	0.53	1.62
V_C3	0.20	0.65	0.85	1.31
V_C4	0.20	0.98	1.18	1.21
V_C5	0.20	1.46	1.66	1.14

Table 2: Evaluation of different contraction heights of the Venturi-shaped windexchanger: volumetric flow rate, Q; and volumetric flow rate percentage where the RC is taken as reference for comparison, Q'.The reference case is indicated in bold.

Cases	Q [m^3/s]	Q' [%]
RC	**3.24** $\times 10^{-1}$	**100**
V_C1	2.68 $\times 10^{-1}$	83
V_C2	3.04 $\times 10^{-1}$	94
V_C3	3.41 $\times 10^{-1}$	105
V_C4	3.58 $\times 10^{-1}$	111
V_C5	3.50 $\times 10^{-1}$	108

VESWE roof thickness

In Figure 7, the VESWE with the optimal c, *i.e.* V_C4, with different thickness of roof, e, U_m/U_{ref} and Cp are shown, together that of the RC. The values of Q and Q' for these cases are presented in Table 3. The case V_C4_e40 improves the Q in 12% with respect of the RC. This behavior is an indication that the VESWE geometry has a complex interaction with the window at windward.

DISCUSSIONS AND CONCLUSIONS

The goal of this work is numerically evaluate the natural ventilation improvement of a room with a window at windward and with a Venturi-shaped windexchanger (VESWE) with respect to a similar windexchanger with flat roof. The CFD simulations are performed for an specific VESWE geometrical configuration, *i.e.* square-cross-section, one duct, with four openings, and located at the center of the roof of an isolated specific room with a window at windward, and the incidence wind normal to one of the VESWE openings. For these conditions, it is

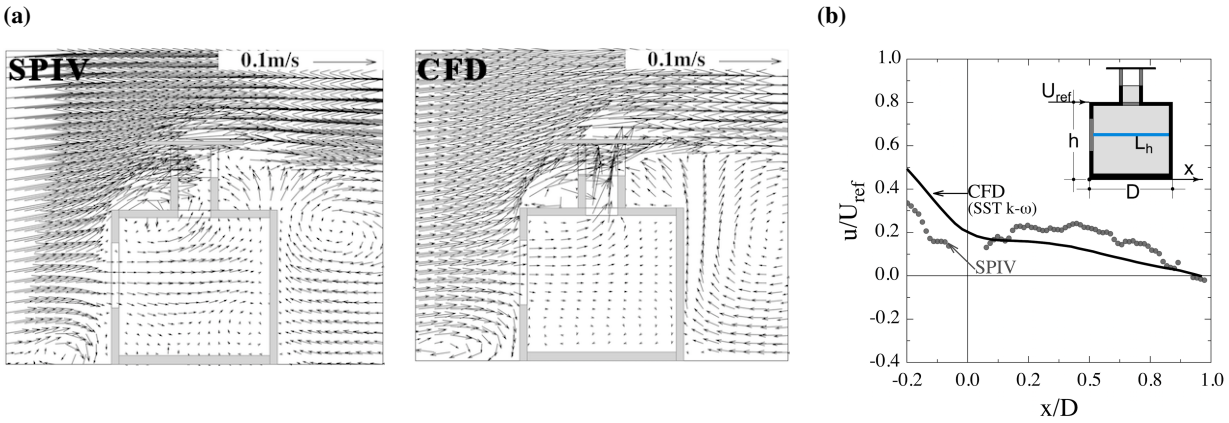

Figure 4: Experimental (SPIV) and numerical (CFD) results: (a) Velocity vector field at the central plane and (b) Streamwise speed ratio u/U_{ref} along the central line L_h.

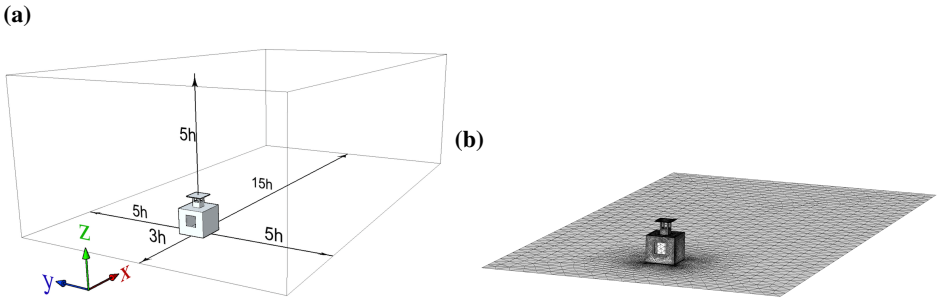

Figure 5: Computational domain extended to analyze the effect of the Venturi-shaped windexchanger: (a) Perspective view of the room in its computational domain. (b) View of the computational grid (room and ground).

Table 3: Evaluation of different roof thickness of the Venturi-shaped windexchanger: volumetric flow rate, Q; and volumetric flow rate percentage where the RC is taken as reference for comparison, Q′.The reference case is indicated in bold.

Cases	Q **[m^3/s]**	Q' **[%]**
RC	**3.24** $\times 10^{-1}$	**100**
V_C4_e10	3.48 $\times 10^{-1}$	107
V_C4_e20	3.58 $\times 10^{-1}$	111
V_C4_e30	3.58 $\times 10^{-1}$	111
V_C4_e40	3.63 $\times 10^{-1}$	112
V_C4_e50	3.48 $\times 10^{-1}$	108

concluded that there exist an optimal height of the contraction of the VESWE that gives the larger volumetric flow rate, due to the competition of the Venturi and wind-blocking effects. The variation of the roof thickness of the VESWE does not give a so clear result, showing that the VESWE geometry has a complex interaction with the window at windward. The volumetric flow rate can increase up to 12% with respect to the similar WE with flat roof.

Further research has to be perform to expand the present work. Some of the issues that must be addressed are: other the orientations and size of the room window, other wind incidence angles, other shapes of the Venturi-shaped roof, and the combination of the wind with thermal effects.

ACKNOWLEDGMENT

This work has been partially supported by the PAPIIT-UNAM IN113314 project. J.A. Castillo acknowledge the scholarship by the CONACYT 235382 grant.

REFERENCES

Bañuelos Ruedas, F., C. Angeles-Camacho, and S. Rios-Marcuello. 2010. "Analysis and validation of the methodology used in the extrapolation of wind speed data at different heights." *Renewable and Sustainable Energy Reviews* 14 (8): 2383–2391.

Blocken, B., T. Stathopoulos, and J. Carmeliet. 2008. "A numerical study on the existence of the Venturi-effect in passages between perpendicular buildings." *Journal of Engineering Mechanics ASCE* 12 (134): 1021–1028.

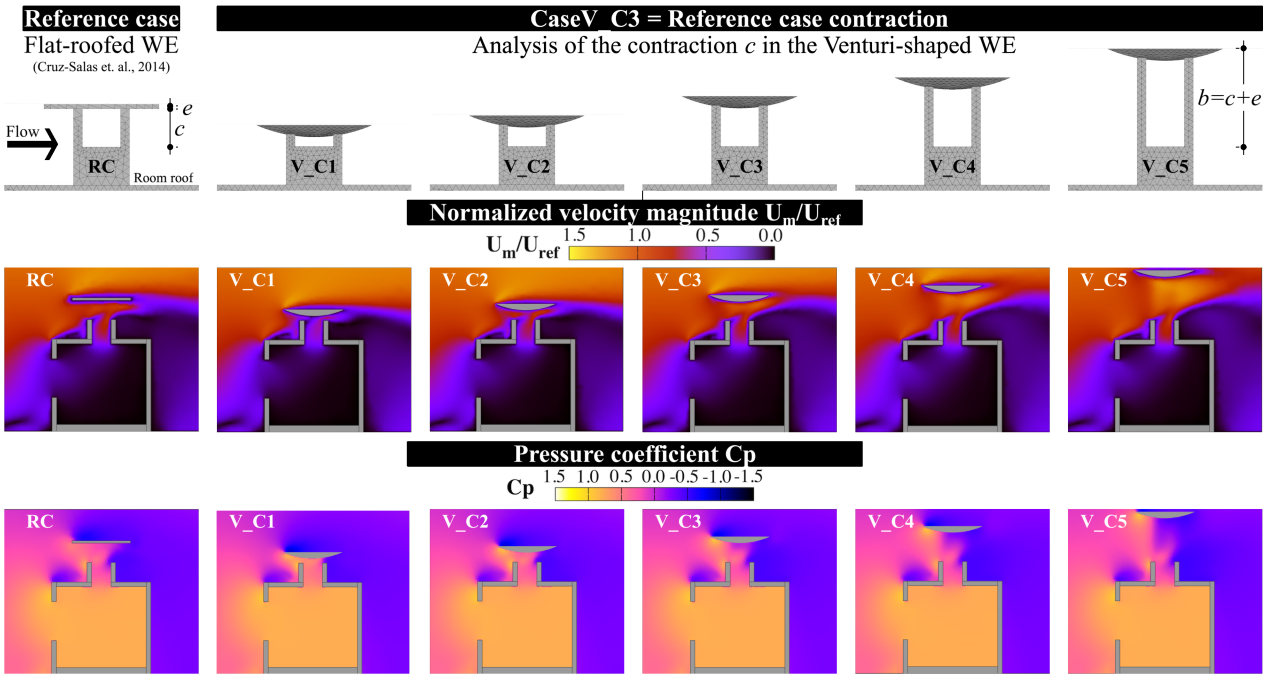

Figure 6: Vertical cross-section of the computational grid for VESWE height contractions, c. The variables e and $b = c + e$ indicate the roof thickness and the height from the WE sill to the WE rooftop, respectively.

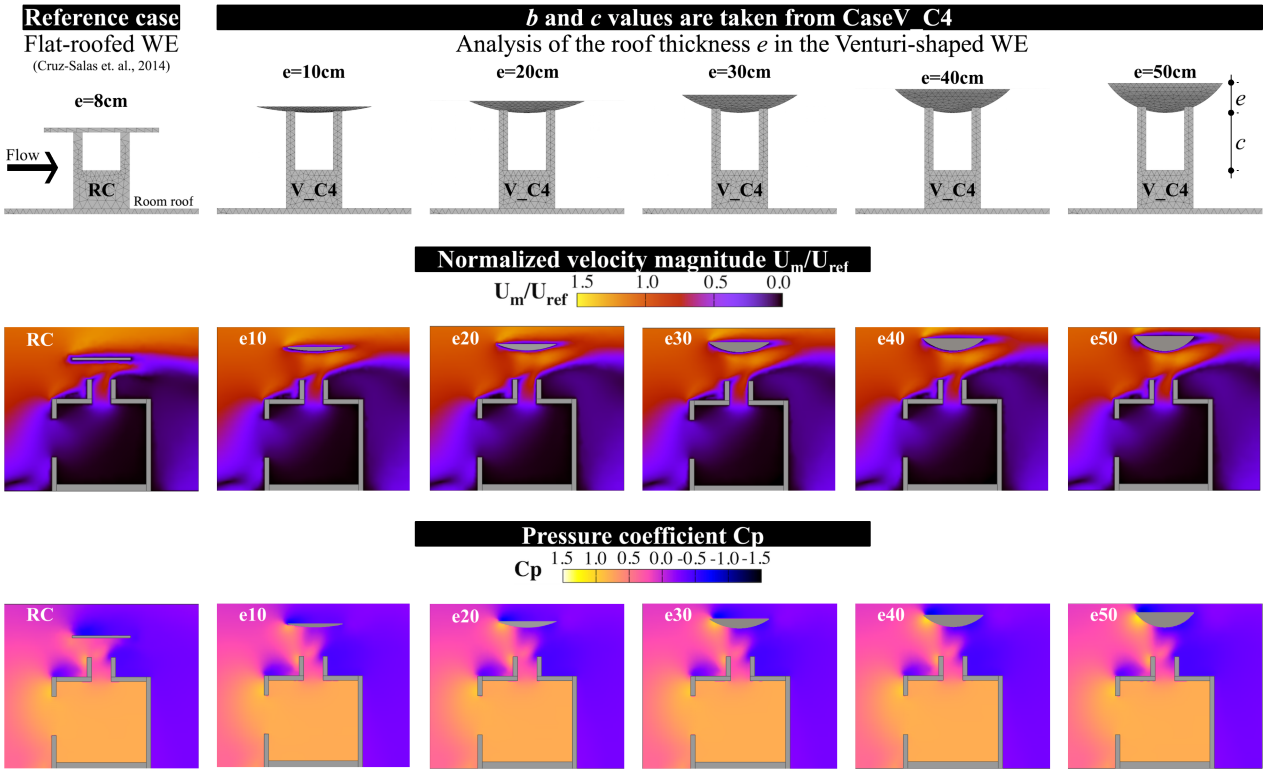

Figure 7: Vertical cross-section of the computational grid for VESWE roof thickness, e. The height from the WE sill to the WE rooftop c is constant for all the VESWE cases.

Blocken, B., T. van Hooff, L. Aanen, and B. Bronsema. 2011. "Computational analysis of the performance of a venturi-shaped roof for natural ventilation: Venturi-effect versus wind-blocking effect." *Computers and Fluids* 48 (1): 202–213.

Bronsema, B, ed. 2010. *Earth, wind and fire air-conditioning powered by nature*. 10th REHVA world congress CLIMA 2010, Antalya, Turkey.

Castillo, J. A., G. Huelsz, and M. V. Cruz, eds. 2014. *Natural ventilation by windcatchers: CFD simulations and experiments*. CWE 2014, 6th International Symposium on Computational Wind Engineering, Hamburg, Germany.

COMSOL. 2013. *COMSOL module CFD user guide*. U.S.: COMSOL AB.

Cruz-Salas, M.V., J. A. Castillo, and G. Huelsz. 2014. "Experimental study on natural ventilation of a room with a windward window and different windexchangers." *Energy and Buildings* 84:458–465.

Elmualim, A. A. 2006a. "Dynamic modelling of a wind catcher/tower turret for natural ventilation." *Building Services Engineering Research and Technology* 27 (3): 165–182.

Elmualim, A. A., and H. B. Awbi. 2002. "Wind tunnel and CFD investigation of the performance of windcatcher ventilation systems." *International Journal of Ventilation* 1 (1): 53–64.

Elmualim, A.A. 2006b. "Effect of damper and heat source on wind catcher natural ventilation performance." *Energy and Buildings* 38:939–948.

Etheridge, D. 2012. *Natural ventilation of buildings – Theory, measurement and desing*. Chichester: Johh Wiley and Sons.

Franke, J., A. Hellsten, H. Schlünzen, and B. Carissimo. 2007. "Best practice guideline for the CFD simulation of flows in the urban environment." *COST office*.

Hughes, B. R., and S. A. A. A. Ghani. 2010. "A numerical investigation into the effect of Windvent louvre external angle on passive stack ventilation performance." *Building and Environment* 45 (4): 1025–1036.

Khan, N., Y. Su, and S. B. Riffat. 2008. "A review on wind driven ventilation techniques." *Energy and Buildings* 40 (8): 1586–1604.

Khodakarami, J., and M. R. Aboseba. 2015. "Impact of openings' number and outdoor flow direction on the indoor vertical flow velocity in wind catchers." *International Journal of Renewable Energy Research* 5 (2): 325–333.

Li, L., and C. M. Mak. 2007. "The assessment of the performance of a windcatcher system using computation fluid dynamics." *Building and Environment* 42 (3): 1135–1141.

Liu, S., C. M. Mak, and J. Niu. 2011. "Numerical evaluation of louver configuration and ventilation strategies for the windcatcher system." *Building and Environment* 46 (8): 1600–1616.

Montazeri, H. 2011. "Experimental and numerical study on natural ventilation performance of various multi-opening wind catchers." *Building and Environment* 46 (-): 370–378.

Montazeri, H., and R. Azizian. 2008. "Experimental study on natural ventilation performance of one-sided wind catcher." *Building and Environment* 43:2193–2202.

Montazeri, H., F. Montazeri, R. Azizian, and S. Mostafavi. 2010. "Two-sided wind catcher performance evaluation using experimental, numerical and analytical modeling." *Renewable Energy* 35:1424–1435.

Partridge, J.L., and P.F. Linden. 2013. "Validity of thermally-driven small-scale ventilated filling box models." *Experiments in Fluids* 54:1–9.

Ramponi, R., and B. Blocken. 2012. "CFD simulation of cross-ventilation for a generic isolated building: Impact of computational parameters." *Building and Environment* 53:34–48.

Saadatian, O., L. C. Haw, K. Sopian, and M. Y. Sulaiman. 2012. "Review of windcatcher technologies." *Renewable and Sustainable Energy Reviews* 16 (3): 1477–1495.

Su, Y., S. B. Riffat, Y. Lin, and N. Khan. 2008. "Experimental and CFD study of ventilation flow rate of a Monodraught windcatcher." *Energy and Buildings* 40 (6): 1110–1116.

Tominaga, Y., A. Mochida, R. Yoshie, H. Kataoka, T. Nozu, and M. Yoshikaw. 2008. "AIJ guidelines for practical applications of CFD to pedestrian wind environment around buildings." *Journal of Wind Engineering and Industrial Aerodynamics* 96:1749–1761.

van Hooff, T., B Blocken, A Aanen, and B Bronsema. 2011. "A venturi-shaped roof for wind-induced natural ventilation of buildings: Wind tunnel and CFD evaluation of different design configurations." *Building and Environment* 46:1797–1807.

Wieringa, Jon. 1992. "Updating the Davenport roughness classification." *Journal of Wind Engineering and Industrial Aerodynamics* 41:357 – 368.